Scientific Research Publishing

World Journal of Nuclear Science and Technology, 2022, 12, 88-100
https://www.scirp.org/journal/wjnst
ISSN Online: 2161-6809
ISSN Print: 2161-6795

Competition of Electron Capture and Beta Decay Rates in Explosive Astrophysical Scenario of Type II Supernova

Rulee Baruah[1], Kalpana Duorah[2], Hira Lal Duorah[2]

[1]Department of Physics, HRH The Prince of Wales Institute of Engineering and Technology, Jorhat, India
[2]Department of Physics, Gauhati University, Guwahati, India
Email: ruleeb@yahoo.com

How to cite this paper: Baruah, R., Duorah, K. and Duorah, H.L. (2022) Competition of Electron Capture and Beta Decay Rates in Explosive Astrophysical Scenario of Type II Supernova. *World Journal of Nuclear Science and Technology*, **12**, 88-100.
https://doi.org/10.4236/wjnst.2022.122008

Received: February 10, 2022
Accepted: April 26, 2022
Published: April 29, 2022

Abstract

Stellar weak interaction processes play a significant role during the supernova explosion condition after collapse leading to the formation of neutron star. In dynamic events like core-collapse supernovae the high entropy wind scenario arises from considerations of the newly born proto-neutron star. Here, the late neutrinos interact with matter of the outermost neutron star layers leading to moderately neutron rich ejecta. We study the electron capture and beta decay rates of Co and Cd isotopes at various temperature and density conditions in an astrophysical environment and found that the beta decay rates are much higher than the corresponding electron capture rates at all the conditions.

Keywords

Protoneutron Star, Weak Interaction Processes, Neutrinos

1. Introduction

The r-process (rapid neutron capture process) nucleosynthesis is traditionally considered to be responsible for synthesis of most of the heavy elements beyond iron [1] and is the only process to produce the naturally occurring radioactive actinide elements like Th and U [2] [3]. Though the site of the r-process is still not clearly known, it has been proposed that explosive and dynamic astrophysical environment of core collapse type II supernova is a viable site [4] [5].

Various weak interaction processes, chiefly electron capture and beta decay play a crucial role during the late stage of stellar burning and subsequent gravitational collapse for a type II supernova. The late stages stellar evolution of mas-

sive stars is strongly influenced by the weak interactions which act to determine the core entropy and electron-to-baryon ratio, Y_e, of the presupernova star [6]. When electron capture reduces the number of electrons available for pressure support, the beta decay acts in the opposite direction. But both the processes generate neutrinos. After collapse the bounce pushes the material outward in form of shock wave where the energy of neutrinos eventually causes the explosion. The outward propagation of the shock depends on the rates of these processes. For most of the heavy and superheavy elements produced here, the experimental information is largely scarce and hence collecting information about the elements gets prohibited [7]. Also it has been identified that the difficulty to pinpoint the r-process site is the lack of experimental data for the relevant nuclei [3]. So a theoretical approach is considered a first step for gathering information on the nuclei produced in such environments.

We organize our work as follows. In Section 2 we make a brief literature review of the nucleosynthesis process in supernova. In Section 3 we discuss these weak interaction processes. Section 4 deals with the calculation of electron capture rates. In Section 5 we present and discuss the comparison of electron capture and beta decay rates of some isotopes of Co and Cd at dynamic explosive scenario of type II supernova. The electron capture rate on ^{59}Co arguably plays a pivotal role in the presupernova evolution of massive stars [8]. ^{130}Cd is a typical r-process element [4] and also $_{48}Cd$ is presumably the most important waiting point isotope for the main r-process. Hence these two isotopes are considered for analysis of weak interaction processes of particular isotopes. For simulation of core collapse of a massive star, the stellar weak interaction rates are considered as one of the most important nuclear physics input parameters [8]. So a calculation of these rates based on a detailed temperature and density scale appropriate to the presupernova and supernova evolution may be an important tool for the simulators of core collapse supernova.

2. Nucleosynthesis in Supernova Type II

2.1. Supernova Core Collapse Mechanism

In the chemical evolution of the Universe, light elements formed after the Big Bang is converted to heavier elements by nuclear fusion in stellar interiors [9]. Due to successive thermonuclear fusion starting from hydrogen, the inner core of a massive star ($M > 10M_0$) exhausts its nuclear fusion fuels at stages and ends up in an iron core which can fuse no further due to large coulomb barrier associated with iron nuclei. The most strongly bound Fe peak nuclei grows larger in mass until a point is reached where the electron degeneracy pressure is no longer able to sustain the core against gravitational collapse [10]. When the core matter exceeds the nuclear matter density (10^{14} gm·cm^{-3}), it collapses catastrophically to form a neutron star or a black hole depending upon the initial contracting mass. In the resulting explosion, the outer layers of the star are blown out where the r-process nucleosynthesis takes place. This is referred to as the supernova explo-

sion which is one of the most probable site of r-process nucleosynthesis.

During the beginning of collapse at high temperature and pressure, the core matter consisting mostly of iron, disintegrates using energy which cools the matter. This is the late stage of stellar burning where in the compact matter the electron capture on protons and nuclei takes place. The reactions are as follows:

$$\mathrm{p} + \mathrm{e}^- \rightarrow \mathrm{n} + \nu_e$$

or on nuclei,

$$(N, Z) + \mathrm{e}^- \rightarrow (N+1, Z-1) + \nu_e$$

As evident from above, these are the reactions which also reduce the electron pressure and enhance neutralization of matter. The neutrinos produced leave the core matter and carry away energy. As the core attains the nuclear matter density and stiffens beyond that, it cannot get compressed further. The still in falling matter is bounced back with the formation of an outward shock, which disintegrates the stellar matter and there is no explosion due to this prompt shock. This neutrino cooling (photodissociation of Fe) competes with neutrino heating (produced by e^- capture) in the stellar matter. The heating causes convective overturn of matter and increases pressure behind the shock which is termed as hot bubble. The persistent neutrino heating drives the shock outward in the form of supernova explosion. The most promising mechanism for SN explosion after iron core collapse of a massive star is the neutrino heating beyond the hot protoneutron star by processes

$$\mathrm{n} + \nu_e \leftrightarrow \mathrm{p} + \mathrm{e}^-$$

$$\nu_e + \mathrm{p} \leftrightarrow \mathrm{n} + \mathrm{e}^+$$

Here at high neutron densities and temperatures, neutron captures and reverse photodisintegrations take place with $\tau_{n,\gamma}$ & $\tau_{\gamma,n} < \tau_\beta$ [11]. It produces the isotopic chain by successive neutron captures before beta decay allows it to move onto the next nucleus so that another isotopic chain can form. Thus β^--decay lifetimes of these nuclei are critical inputs for the r-process because they not only set the timescale for heavy element production but also help to shape the final abundance pattern as the path moves back to stability [5]. In this r-process, finally highly unstable heavy and superheavy nuclei with short half lives are produced. We start with ${}_{26}Fe$ as seed nucleus to produce these heavy elements by r-process nucleosynthesis. We calculate the beta decay rates λ_{β^-} which is related to the half lives of these very neutron rich nuclei via $\lambda_{\beta^-} = \ln 2/T$.

We can see that the electron capture precedes beta decay which is evident from the above discussion. But just after explosion as temperature and density decrease exponentially [12] and r-process nucleosynthesis starts, the beta decay of the nuclei produced increases Y_e, the electron fraction and compete with electron capture.

2.2. R-Process Nucleosynthesis

In the classical r-process under conditions of high temperature ($T_9 > 1$, $T_9 = 10^9$

K) and high neutron number density ($n_n > 10^{20}$ cm^{-3}), a nucleus can capture neutrons successively and as permitted by the neutron binding energy of that nucleus. This we calculate from Saha equilibrium on nuclei in a certain isotopic chain [13] given as

$$S_n \approx \left[34 - \log_{10}\left(n_n\right)\right] \times T_9 / 5 \text{ MeV}$$

Here after each neutron capture, the binding energy falls until ultimately the binding becomes zero and a nucleus can further capture no more neutrons. The nucleus then waits until β^--decay allows it to proceed onto the next nucleus and a new chain of isotopes forms.

When the temperature T significantly exceeds T_9 initially, a hot r-process occurs [14]. For T_9 ~2 and $n_n > 10^{20}$ cm^{-3}, photo-disintegration is sufficiently fast to establish an equilibrium with neutron capture. In this (n, γ) ↔ (γ, n) equilibrium, the total abundance of nuclei with a specific Z is concentrated in a waiting point nucleus assigned by relevant n_n and T which provides their neutron separation (binding) energies $S_n(Z, A)$ based mainly on the nuclear masses. From mass considerations the neutron separation energy is given as

$$S_n\left(Z, A\right) = M\left(Z, A-1\right)c^2 + M_n c^2 - M\left(Z, A\right)c^2$$

Nuclear masses here play an important role by also providing the excess neutron binding energy from one neutron to the next. This is calculated from nuclear mass data of [15]. Thus the r-process path formed by the waiting point nuclei is specified by n_n, T and $S_n(Z, A)$. The β^--decay of the waiting point nuclei regulates the relative abundances for different Z and controls the progress of the r-process flow. This is discussed in detail in an earlier paper by these authors [16].

During expansion as the temperature drops below some critical value and free neutrons are depleted at some point, the (n, γ) ↔ (γ, n) equilibrium breaks down. If T is far below T_9 then the r-process takes place in relatively cold environments where the r-process flow is controlled by the individual neutron capture followed by β^--decays both of which play an important role in the final abundances of nuclei. When the neutron source is exhausted, the r-process freezes out and the unstable nuclei decay back to stability. In different isotopic chains, the relative abundances are set by β^--decay lifetimes of the heaviest nuclei along each chain. The chains are connected via β^--decays and thus an r-process path is formed at different temperature and densities of the explosive environment. Along the path the successive β^--decays set the time required to produce the heaviest element possible [17].

Only a small fraction of nuclei involved in r-process are accessible to experiments. So majority of nuclear inputs like temperature, density and mass of nuclei involved are calculated from theory and used in a network of equations to provide the abundances, β^--decay rates and electron capture rates theoretically. Here we adopt a theoretical approach to calculate the weak interaction rates and make a comparison of them in the explosive environment of type II supernova.

3. Stellar Weak Interaction Processes

Stellar weak-interaction processes and their rates exhibit considerable variations because they are extremely sensitive to the dynamic range of density and temperature that occur in the stars; the rates observed also vary a lot than those observed in the terrestrial laboratory. Atoms are generally completely ionized, while electrons form a continuum gas in the stellar plasma [18]. The electron gas has a degree of degeneracy that strongly depends on both the temperature and density of the matter inside a star. During the evolutionary process of a massive star, in the final stage when the central density of the star exceeds the nuclear matter density, electrons exhibit high degeneracy which strongly affects the rates of weak interactions.

3.1. Rates of Weak Interaction in the Stellar Interior

In massive stars during the presupernova evolution, allowed GamowTeller transitions dominate weak interaction processes. The two main weak interaction processes are the electron capture and the β^--decay:

$$e^- + (A,Z) \to (A,Z-1) + \nu_e$$

$$Q_{ec} \approx \left[M(A,Z) - M(A,Z-1)\right]c^2$$

$$(A,Z) \to (A,Z+1) + e^- + \nu_e;$$

$$Q_\beta \approx \left[M(A,Z) - M(A,Z+1)\right]c^2$$

where (A, Z) characterizes a nucleus with mass number A and atomic number Z and has a nuclear mass $M(A, Z)$; Q's are the energy values. As a consequence, the rates of the two major weak-interaction processes during the presupernova evolution in massive stars indicate that β^--decays can compete with e^--captures on nuclei because of the following reasons. That: 1) the e^--capture rates generally decrease as observed in the calculations and 2) the increase in the β^--decay rates owing to thermal excitation of the back resonances and evolution of nuclear matter towards neutron-rich nuclei attained by the r-process. This increase favors the β^--decay processes more than the e^- capture processes because the energy Q_{β^-} decreases while the energy Q_{ec} increases.

3.2. Competition between the Rates of Electron Capture and Beta Decay in a Supernova Collapse

Weak-interaction processes are pivotal to the initial stage of the core collapse of a massive star. When the core mass of the star surpasses the appropriate Chandrasekhar mass limit, the electron capture that is taking place on the nuclei in iron-mass region augments a reduction in the electron pressure. Thus the electron degeneracy pressure which opposes the collapse is dropped down. This accelerates the collapse while simultaneously reducing the electron fraction Y_e [19]. In addition, this alters the distribution of the nuclei existent in the star core increasing the neutron richness of the material. In this stage, many of the nuclei

formed can also undergo β^--decay. Although this process is relatively less crucial than the electron capture for the initial values of Y_e near 0.5, it becomes progressively more competitive for neutron-rich nuclei. The rates of the electron capture and beta decay processes have been found to balance each other within a particular range of Y_e values.

These processes, chiefly electron capture and beta decays, create neutrinos which escape the star continuously for all densities until the collapse becomes truly hydrodynamic (*i.e.* $\rho \sim 10^{11}$ gm·cm^{-3}). Thus, they carr energy away from the star and reduce entropy. During simulations that follow stellar evolution till the iron core attains the central densities of order of a few 10^9 gm·cm^{-3}, the knowledge of average neutrino energies of the various weak processes involved is sufficient for determining the rate of energy loss along the stellar trajectory. These simulations are referred as the pre supernova model, which are then used as an input to carry out the detailed studies on the collapse and explosion mechanisms of stars. [20] suggested that under conditions of the pre-supernova models and in subsequent stellar evolution, the β^--decay is strongly inhibited by the appreciable electron chemical potential. Moreover, the total electron capture rates are some orders of magnitude higher than the beta decay rates. Knowledge of neutrino energy spectra at each point and time during core collapse of a massive star is fairly relevant to simulations of the final collapse and explosion phase of the massive star.

The electron capture and beta decay processes become much significant when nuclei with masses $A \sim 55$ - 60 are most abundant in the core. As weak interaction changes the value of Y_e and electron capture process becomes dominant; the Y_e value is reduced successively from its initial value of 0.5. Consequently, the abundant nuclei become increasingly neutron rich and heavier because nuclei with a low Z/A ratio are more bound in heavier matter than are those with a high Z/A ratio.

4. Calculation of the Electron Capture Rates

Beta interaction rates include electron-antineutrino and positron-neutrino emission, electron capture with neutrino emission and positron capture with antineutrino emission. According to [21], stellar electron capture rates are very sensitive to temperature and density and can differ considerably from terrestrial values for a given transition. Reference [22] pointed out that the excited states of a nucleus may have quite different β^--decay rates than the ground state of the nucleus. Electron capture occurs in stars from bound and continuum orbits and for the nuclei the continuum capture is important under the conditions discussed here.

The allowed differential rate for e^--capture from the energy interval $\mathrm{d}\omega$ in the continuum (subscript c) is given by

$$\mathrm{d}\lambda\left(e_c^-\right) = \sum C^2 \left|M\right|^2 F_- \pi^2 \left(\omega + q_n\right)^2 \left(\frac{\hbar}{m_e c}\right)^3 \frac{\mathrm{d}n_-}{\mathrm{d}\omega} \mathrm{d}\omega \tag{1}$$

Here the effective matrix element squared is given [21] as

$$\sum C^2 |M|^2 = C_V^2 |M_F|^2 + \sum C_A^2 |M_{GT}|^2 \tag{2}$$

where M_F and M_{GT} are Fermi and Gammow Teller nuclear matrix elements and C_V^2 and C_A^2 are constants in units of sec^{-1}. In the non-relativistic limit

$$F_-(z,\omega) = \frac{2\pi\eta}{\left|\exp(-2\pi\eta)-1\right|} \tag{3}$$

where

$$\eta = \frac{Ze^2}{\hbar v} = \alpha Z \frac{c}{v} = \alpha Z \frac{\omega}{p} \tag{4}$$

is the electron or positron momentum in units of $m_e c$, a positive quantity for both electron and positron emission with v the electron or positron velocity, α = 1/137 the fine structure constant, and Z the charge number of the final nucleus. Also $\omega^2 = (\omega + q_n)^2 = (\omega + q_\alpha + 1)^2$ is the energy proportional to the phase space factor for the emitted neutrino or antineutrino. The differential electron density is given by

$$\frac{\mathrm{d}n_-}{\mathrm{d}\omega} = \frac{1}{\pi^2}\left(\frac{m_e c}{\hbar}\right)^3 \left(\frac{v}{c}\right)\omega^2 \exp(-z\omega + \phi) \tag{5}$$

Here, the Fermi-Dirac number density of electrons in equilibrium with the radiation field and with nuclei are

$$n_- = \rho N_- = \frac{1}{\pi^2}\left(\frac{m_e c}{\hbar}\right)^3 \int_0^\infty \frac{\omega(\omega^2-1)^{1/2}\,\mathrm{d}\omega}{\exp(z\omega-\phi)+1} \tag{6}$$

where $z = m_e c^2/kT = 5.930/T_9$, ω is the total energy in units of $m_e c^2$, $\phi = \varphi/kT$ is the chemical potential for electrons in units of kT. With this now,

$$n_- = \rho N_- = n_1 \exp(+\phi) \tag{7}$$

where

$$n_1 = \rho N_1 = \frac{1}{\pi^2}\left(\frac{m_e c}{\hbar}\right)^3 \int_0^\infty \exp(-z\omega)\left(\frac{v}{c}\right)\omega^2 \mathrm{d}\omega \tag{8}$$

Here in the extreme relativistic (ER) non-degenerate case, one has

$$n_1 \approx 1.688\times 10^{28} T_9^3 \ \mathrm{cm}^{-3} \tag{9}$$

When this is done, one has, with $z = m_e c^2/kT$ and $n_-/n_1 = \exp(+\phi)$

$$\mathrm{d}\lambda(e_c^-) = 2\pi\alpha Z \sum C^2 |M|^2 \left(\frac{F_-}{2\pi\eta}\right)\frac{n_-}{n_1}\exp(-z\omega)\omega^2(\omega+q_n)^2\,\mathrm{d}\omega \tag{10}$$

To obtain $\lambda(e_c^-)$, two cases have been distinguished. In the first case $q_n = Q_n/m_e c^2$, is the nuclear energy difference in units of $m_e c^2$ between the capturing state and the final nuclear state which lie in the range $q_n > -1$, so that the range of integration is $1 < \omega < \infty$. In the second case $q_n < -1$, so that the range is $|q_n| < \omega < \infty$. Thus we get

$$\mathrm{d}\lambda\left(e_c^-\right) = \sum C^2 \left|M\right|^2 f\left(e_c^-\right) \tag{11}$$

with

$$f\left(e_c^-\right) = 2\pi\alpha Z \left\langle \frac{F_-}{2\pi\eta} \right\rangle \frac{n_-}{n_1} I_- \tag{12}$$

where Z is the charge number of the initial nucleus and n_1 being given by equation (8). In terms of atomic mass difference $q_n = q - 1$ in the electron capture case and for $q_\alpha > 0$, we have

$$I_- = \frac{\exp(-z)}{z} q_\alpha^2 \left[\left(1 + \frac{2}{z} + \frac{2}{z^2}\right) + 2\left(\frac{kT}{Q_\alpha}\right)\left(1 + \frac{4}{z} + \frac{6}{z^2}\right) + 2\left(\frac{kT}{Q_\alpha}\right)^2 \left(1 + \frac{6}{z} + \frac{12}{z^2}\right) \right] \tag{13}$$

while for $q_\alpha < 0$

$$I_- = \frac{2\exp\left(-z + \left|Q_\alpha / kT\right|\right)}{z^3} \left|q_\alpha\right|^2 \left[1 + \left|\frac{2}{q_\alpha}\right| \left(1 + \frac{3}{z}\right) + \left|\frac{1}{q_\alpha}\right|^2 \left(1 + \frac{6}{z} + \frac{12}{z^2}\right) \right] \tag{14}$$

In order to express the continuum capture rates numerically, taking $Q_\alpha = Q_n + 0.511$ MeV > 0 and $\langle F_-/2\pi\eta \geq 1.6$ we finally have

$$\lambda\left(e_c^-\right) = 2.76 \times 10^{-5} Z \left|M\right|^2 \left(Q_\alpha^2 + 1.26 Q_\alpha + 0.665\right) \tag{15}$$

For allowed transitions near $Z = 26$, we have according to [21], $|M|^2 = 0.5$ to 0.01.

5. Results and Discussion

It has been proved that the dynamical timescale of the final collapse is dominated by electron capture on nuclei and not, as has been the standard picture for many years, by capture on free protons. This has a significant consequence for the collapse and changes the Y_e and density profiles throughout the core.

The treatment of [21] has been followed and the electron capture rates for ^{55}Co iso tope at various arbitrary values of $|M|^2$ are calculated. These rates (henceforth referred as FH rate) are compared with that of [19] at the same temperature and density conditions and are tabulated in **Table 1**. The rates indicated are shell-model (SM), Fuller, Fowler and Newman (FFN) and Aufder-heide *et al.* (Aufd), all the values being taken from [19].

It is noted that the value of $|M|^2 = 0.03$ gives the e^--capture rates of FH much in agreement with that of others, as shown in **Table 1**. So, we now propose that this $|M|^2 = 0.03$ value be taken in calculating the e^--capture rates at different temperature and density conditions considered in the present analysis by using equation (15) and then compare them with the β^--decay rates of our calculation [16]. These are shown in **Figure 1** for $_{27}Co$ isotopes and in **Figure 2** for $_{48}Cd$ isotopes. $_{48}Cd$ is presumably the most important "waiting-point" isotope for the main r-process and hence it is taken for the analysis. It is found that the β^--decay rates are much higher than the corresponding e^--capture rates at all the conditions. As the temperature increases which also indicates an increased density, we

Table 1. Electron capture rates for ^{55}Co isotope at different values of $|M|^2$.

SM	FFN	Aufd	FH	$\|M\|^2$
2.2 (−3)	8.4 (−2)	5.1 (−2)	1.0 (−4)	0.01
1.5 (−4)	1.9 (−3)	3.4 (−3)	1.2 (−4)	
8.7 (−6)	2.1 (−4)	2.1 (−4)	7.9 (−5)	
1.7 (−3)	6.9 (−2)	5.1 (−2)	7.9 (−5)	
3.3 (−4)	9.1 (−3)	2.1 (−2)	7.9 (−5)	
1.8 (−4)	1.1 (−1)	6.1 (−2)	8.0 (−5)	
2.2 (−3)	8.4 (−2)	5.1 (−2)	2.1 (−4)	0.02
1.5 (−4)	1.9 (−3)	3.4 (−3)	2.4 (−4)	
8.7 (−6)	2.1 (−4)	2.1 (−4)	1.6 (−4)	
1.7 (−3)	6.9 (−2)	5.1 (−2)	1.6 (−4)	
3.3 (−4)	9.1 (−3)	2.1 (−2)	1.6 (−4)	
1.8 (−4)	1.1 (−1)	6.1 (−2)	1.6 (−4)	
2.2 (−3)	8.4 (−2)	5.1 (−2)	3.1 (−4)	0.03
1.5 (−4)	1.9 (−3)	3.4 (−3)	3.5 (−4)	
8.7 (−6)	2.1 (−4)	2.1 (−4)	2.4 (−4)	
1.7 (−3)	6.9 (−2)	5.1 (−2)	2.4 (−4)	
3.3 (−4)	9.1 (−3)	2.1 (−2)	2.4 (−4)	
1.8 (−4)	1.1 (−1)	6.1 (−2)	2.4 (−4)	
2.2 (−3)	8.4 (−2)	5.1 (−2)	4.2 (−4)	0.04
1.5 (−4)	1.9 (−3)	3.4 (−3)	4.8 (−4)	
8.7 (−6)	2.1 (−4)	2.1 (−4)	3.2 (−4)	
1.7 (−3)	6.9 (−2)	5.1 (−2)	3.2 (−4)	
3.3 (−4)	9.1 (−3)	2.1 (−2)	3.2 (−4)	
1.8 (−4)	1.1 (−1)	6.1 (−2)	3.2 (−4)	
2.2 (−3)	8.4 (−2)	5.1 (−2)	6.2 (−4)	0.06
1.5 (−4)	1.9 (−3)	3.4 (−3)	7.1 (−4)	
8.7 (−6)	2.1 (−4)	2.1 (−4)	4.8 (−4)	
1.7 (−3)	6.9 (−2)	5.1 (−2)	4.8 (−4)	
3.3 (−4)	9.1 (−3)	2.1 (−2)	4.8 (−4)	
1.8 (−4)	1.1 (−1)	6.1 (−2)	4.8 (−4)	
2.2 (−3)	8.4 (−2)	5.1 (−2)	8.3 (−4)	0.08
1.5 (−4)	1.9 (−3)	3.4 (−3)	9.4 (−4)	
8.7 (−6)	2.1 (−4)	2.1 (−4)	6.4 (−4)	
1.7 (−3)	6.9 (−2)	5.1 (−2)	6.4 (−4)	
3.3 (−4)	9.1 (−3)	2.1 (−2)	6.4 (−4)	
1.8 (−4)	1.1 (−1)	6.1 (−2)	6.4 (−4)	
2.2 (−3)	8.4 (−2)	5.1 (−2)	10.3 (−4)	0.10
1.5 (−4)	1.9 (−3)	3.4 (−3)	11.7 (−4)	
8.7 (−6)	2.1 (−4)	2.1 (−4)	8.0 (−4)	
1.7 (−3)	6.9 (−2)	5.1 (−2)	8.0 (−4)	
3.3 (−4)	9.1 (−3)	2.1 (−2)	8.0 (−4)	
1.8 (−4)	1.1 (−1)	6.1 (−2)	8.0 (−4)	

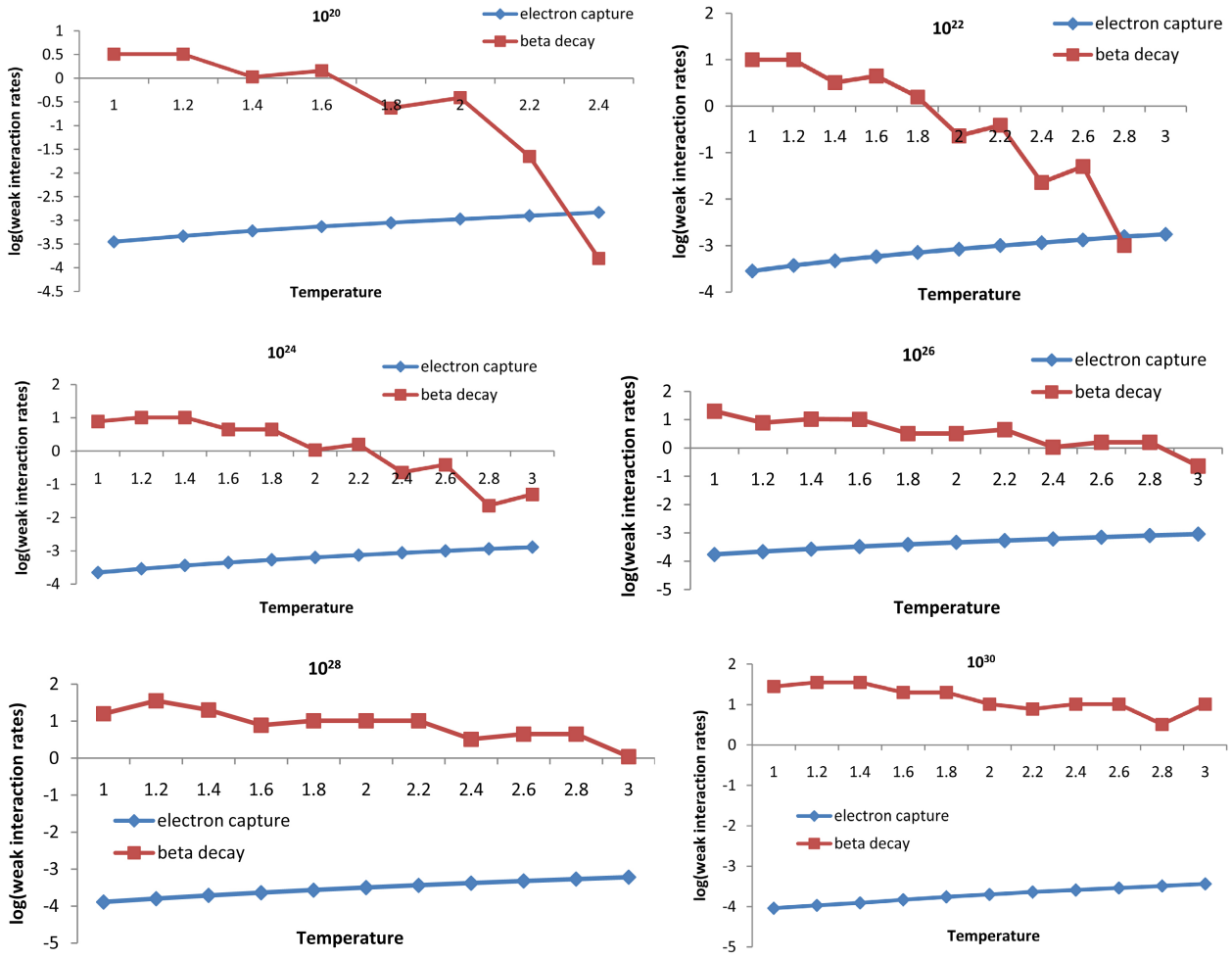

Figure 1. Comparison of the ϵ^--capture and β^--decay rates for $27Co$ isotopes at Temperature and Density Conditions as Specified: rates are in sec^{-1}.

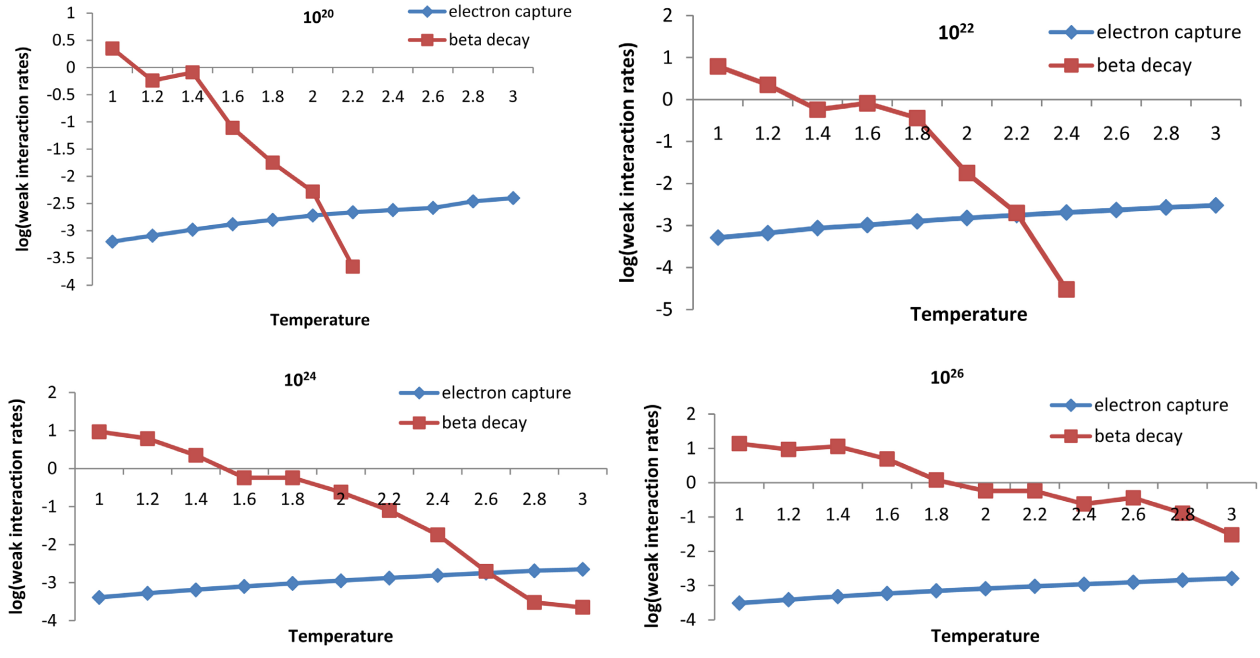

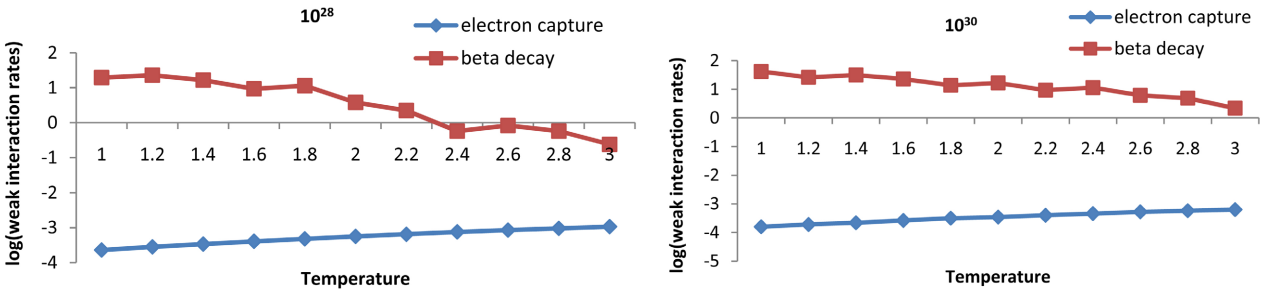

Figure 2. Comparison of the e^--capture and β^--decay rates for 48*Cd* isotopes at Temperature and Density Conditions as Specified: rates are in sec^{-1}.

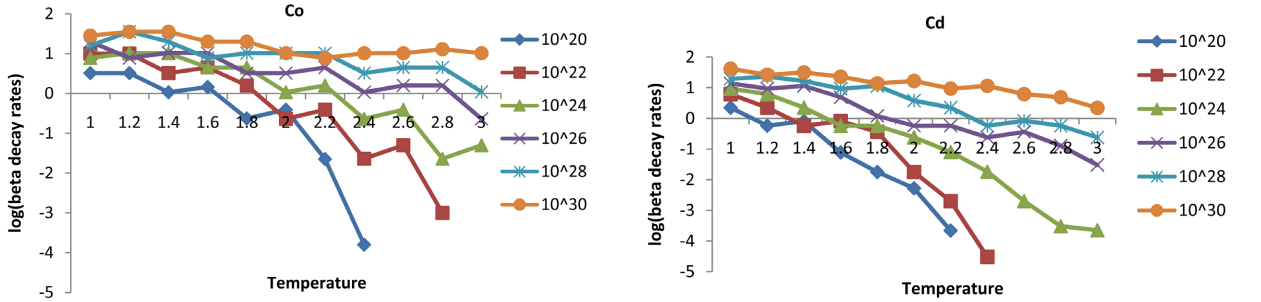

Figure 3. Beta decay rates of Co and Cd isotopes at different temperatures: rates are in sec^{-1}. It is noted that at the same density with the increase in temperature the beta decay rates go on decreasing. Also at the same temperature with the increase in density the beta decay rates go on increasing.

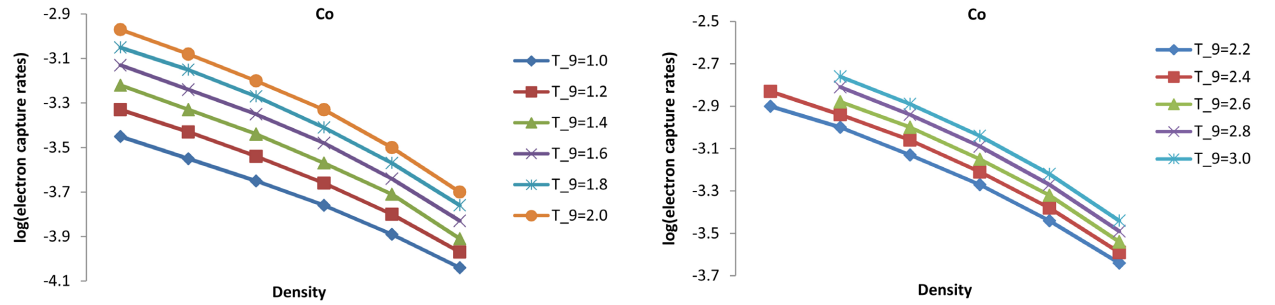

Figure 4. Electron capture rates of Co isotopes at different densities: rates are in sec^{-1}. It is noted that at the same temperature with the increase in density the electron capture rates go on decreasing. Also at the same density with the increase in temperature the electron capture rates go on increasing.

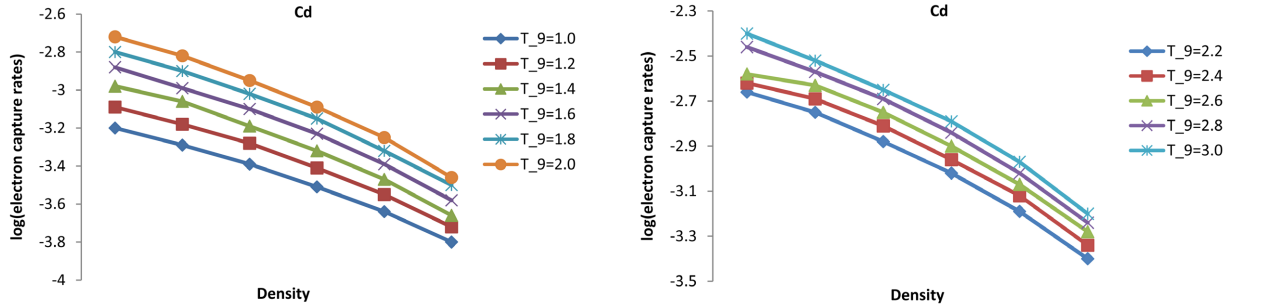

Figure 5. Electron capture rates of Cd isotopes at different densities: rates are in sec^{-1}. It is noted that at the same temperature with the increase in density the electron capture rates go on decreasing. Also at the same density with the increase in temperature the electron capture rates go on increasing.

can see that the electron capture rates go on increasing. This is due to the fact that in the more compact matter the mean free path of the electrons decreases and there is an enhancement of electron capture.

Figure 3 shows the beta decay rates at various density and temperature conditions. It is seen that at the same density with the increase in temperature the beta decay rates go on decreasing. Also at the same temperature with the increase in density the beta decay rates go on increasing. These implications of entropy values will be discussed in detail in our next paper. The figure shows that at high temperature and low density (high entropy, $S(4/3)a(kT)^3/\rho N_A$) conditions, the β^--decay rate is considerably lower (Figure 4 and Figure 5).

Acknowledgements

The authors are extremely thankful to Prof K. L. Kratz for his valuable discussions and suggestions during the preparation of the paper. We are thankful to the Government of Assam for giving the permission to carry out the research work. Grateful thanks are due to Dr. Debasish Bora of IIT, Guwahati for his valuable suggestions on the paper.

Conflicts of Interest

The authors declare no conflicts of interest regarding the publication of this paper.

References

[1] Burbidge, E.M., Burbidge, G.R., Fowler, W.A. and Hoyle, F. (1957) Synthesis of the Elements in Stars. *Reviews of Modern Physics*, **29**, 547-650. https://doi.org/10.1103/RevModPhys.29.547

[2] Wehmeyer, B., Pignatari, M. and Thielemann, F.-K. (2015) Galactic Evolution of Rapid Neutron Capture Process Abundances: The Inhomogeneous Approach. *Monthly Notices of the Royal Astronomical Society*, **452**, 1970-1981. https://doi.org/10.1093/mnras/stv1352

[3] Kajino, T. and Mathews, G.J. (2016) Impact of New Data for Neutron-Rich Heavy Nuclei on Theoretical Models for r-Process Nucleosynthesis. https://arxiv.org/pdf/1610.07929.pdf

[4] Meyer, B.S., McLaughlin, G.C. and Fuller, G.M. (1998) Neutrino Capture and *r*-Process Nucleosynthesis. *Physical Review C*, **58**, 3696-3710. https://doi.org/10.1103/PhysRevC.58.3696

[5] Mumpower, M.R., Surman, R., McLaughlin, G.C. and Aprahamian, A. (2016) The Impact of Individual Nuclear Properties on r-Process Nucleosynthesis. *Progress in Particle and Nuclear Physics*, **86**, 86-126. https://doi.org/10.1016/j.ppnp.2015.09.001

[6] Heger, A., Woosley, S.E., Martınez-Pinedo, G. and Langanke, K. (2001) Presupernova Evolution with Improved Rates for Weak Interactions. *The Astrophysical Journal*, **560**, 307. https://doi.org/10.1086/324092

[7] Kar, K., Chakravarti, S. and Manfredi, V.R. (2006) Beta Decay Rates for Nuclei with 115<A<140 for *r*-Process Nucleosynthesis. *Pramana*, **67**, 363-368. https://doi.org/10.1007/s12043-006-0081-2

[8] Rahman, M.-U. and Nabi, J.-U. (2014) Electron Capture Strength on Odd-A Nucleus ^{59}Co in Explosive Astrophysical Environment. *Astrophysics and Space Science*, **351**, 235-242. https://doi.org/10.1007/s10509-014-1831-0

[9] Buragohain, M., Pathak, A., Sarre, P., Onaka, T. and Sakon, I. (2015) Theoretical Study of Deuteronated PAHs as Carriers for IR Emission Features in the ISM. *Monthly Notices of the Royal Astronomical Society*, **454**, 193-204. https://doi.org/10.1093/mnras/stv1946

[10] Cooperstein, J. and Wambach, J. (1984) Electron Capture in Stellar Collapse. *Nuclear Physics A*, **420**, 591-620. https://doi.org/10.1016/0375-9474(84)90673-0

[11] Thielemann, F.-K., Kolbe, E., Martinez-Pinedo, G., Panov, I., Rauscher, T., Kratz, K., Pfeiffer, B. and Rosswog, S. (2003) Nuclear Physics Issues of the r-Process. In: *Capture Gamma-Ray Spectroscopy and Related Topics*, World Scientific Publishing, Singapore, 311. https://www.worldscientific.com/doi/pdf/10.1142/9789812795151_fmatter

[12] Schramm, D.N. (1973) Explosive r-Process Nucleosynthesis. In: Schramm, D.N. and Arnett, W.D., Eds., *Explosive Nucleosynthesis*, University of Texas Press, Austin, 84. https://ui.adsabs.harvard.edu/abs/1973ApJ...185..293S/abstract

[13] Takahashi, K., Witti, J. and Janka, H.-T. (1994) Nucleosynthesis in Neutrino-Driven Winds from Protoneutron Stars II. The r-Process. *A&A*, **286**, 857. https://ui.adsabs.harvard.edu/abs/1994A%26A...286..857T/abstract

[14] Qian, Y.-Z. (2012) Astrophysical Models of r-Process Nucleosynthesis: An Update. In *Origin of Matter and Evolution of Galaxies* 2011, AIP Conference Proceedings, 201-208. https://doi.org/10.1063/1.4763396

[15] Audi, G., Wapstra, A.H. and Thibault, C. (2003) The Ame2003 Atomic Mass Evaluation: (II). Tables, Graphs and References. *Nuclear Physics A*, **729**, 337-676. https://doi.org/10.1016/j.nuclphysa.2003.11.003

[16] Baruah, R., Duorah, K. and Duorah, H.L. (2012) Isotopic r-Process Abundances Produced by Supernova Explosions. *Astrophysics and Space Science*, **340**, 291-305. https://doi.org/10.1007/s10509-012-1064-z

[17] Cass, J., Passucci, G., Surman, R. and Aprahamian, A. (2012) Beta Decay and the r-Process. *Proceedings of Science*, **146**. https://doi.org/10.22323/1.146.0154

[18] Sampaio, J.M., Langanke, K., Martınez-Pinedo, G., Kolbe, E. and Dean, D.J. (2003) Electron Capture Rates for Core Collapse Supernovae. *Nuclear Physics A*, **718**, 440-442. https://doi.org/10.1016/S0375-9474(03)00832-7

[19] Martınez-Pinedo, G., Langanke, K. and Dean, D.J. (2000) Competition of Electron Capture and Beta-Decay Rates in Supernova Collapse. *The Astrophysical Journal Supplement Series*, **126**, 493. https://doi.org/10.1086/313297

[20] Langanke, K., Martınez-Pinedo, G. and Sampaio, J.M. (2001) Neutrino Spectra from Stellar Electron Capture. *Physical Review*, **64**, Article ID: 055801. https://doi.org/10.1103/PhysRevC.64.055801

[21] Fowler, W.A. and Hoyle, F. (1965) Nucleosynthesis in Massive Stars and Supernovae.

[22] Cameron, A.G.W. (1959) Photobeta Reactions in Stellar Interiors. *Astrophysical Journal*, **130**, 452. https://doi.org/10.1086/146735